AN ANALYSIS OF JET STREAM STRUCTURE AND ENERGETICS USING AN OBJECTIVE COMPUTATIONAL SCHEME

by

Robert Frederick Riordan

United States Naval Postgraduate School

THESIS

AN ANALYSIS OF JET STREAM STRUCTURE AND ENERGETICS
USING AN OBJECTIVE COMPUTATIONAL SCHEME

by

Robert Frederick Riordan

March 1971

Approved for public release; distribution unlimited.

T137642

Thesis R5728
c.1

An Analysis of Jet Stream Structure and Energetics Using an Objective Computational Scheme

by

Robert Frederick Riordan
Lieutenant, United States Navy
B.S., United States Naval Academy, 1964

Submitted in partial fulfillment of the
requirements for the degree of

MASTER OF SCIENCE IN METEOROLOGY

from the

NAVAL POSTGRADUATE SCHOOL
March 1971

ABSTRACT

An analysis of jet stream structure and energetics is performed utilizing an objective scheme that calculates wind components normal and parallel to the jet axis, with provisions to explicitly calculate the eddy components of variables. Most of the meteorological data used is generated by a diagnostic-balanced, ω-equation model. Results indicate that above 500 mb observed winds and temperatures should be used versus computer generated data.

There is some indication that between the jet entrance and exit regions the mean transverse vertical circulation reverses from thermally direct to thermally indirect. Kinetic energy is imported from below the jet into the jet stream region primarily by the mean pressure interaction at 500 mb.

Thermal balance calculations indicate that the mean horizontal temperature advection and vertical transverse motion are primarily responsible for maintenance of the temperature structure about a jet.

TABLE OF CONTENTS

		Page
I.	INTRODUCTION	9
II.	RESEARCH PROCEDURES	13
	A. DESCRIPTION OF JET STREAM COORDINATE SYSTEM	13
	B. METEOROLOGICAL DATA USED	13
	C. DESCRIPTION OF JET STREAM AXES ANALYZED	17
	D. DESCRIPTION OF OBJECTIVE COMPUTATIONAL SCHEME	19
III.	EQUATIONS	21
IV.	RESULTS	25
	A. COMPARISON OF INTERPOLATION METHODS	25
	B. KINETIC ENERGY CALCULATIONS FOR 300 MB JET AXES	29
	C. KINETIC ENERGY CALCULATIONS FOR 200 MB JET AXES	33
	D. ANALYSIS OF AN INDIVIDUAL JET STREAM AXIS	35
	E. INVESTIGATION OF EDDY HEAT FLUX	42
V.	CONCLUSIONS	47
APPENDIX A		49
BIBLIOGRAPHY		54
INITIAL DISTRIBUTION LIST		55
FORM DD 1473		56

LIST OF TABLES

TABLE		Page
1	Mahlman's results vs. computational schemes results of the contribution of terms in the kinetic energy balance equation, Eqn. (4).	31
2	Results of kinetic energy calculations using Eqn. (4) averaged over five days for jet axes defined from balanced winds.	34
3	Kinetic energy calculations using Eqn. (4) for 16 November 1200 GMT jet stream, defined from balanced winds.	40

LIST OF ILLUSTRATIONS

FIGURE		Page
1	Curvilinear grid for jet stream of 15 November 1200 GMT, 1966	14
2	Geopotential heights at 300 mb on 15 November 1200 GMT, 1966	14
3	Jet stream axes at 300 mb, defined the observed winds	18
4	Jet stream axes at 200 mb, defined from the total balanced winds	18
5	Comparison of mean vertical motions interpolated by the objective computational scheme vs. by hand	26
6	Mean wind and temperature by objective computational scheme	27
7	Mean wind and temperature calculated by hand	28
8	Mean vertical motion with respect to e the axis for 16 November 1200 GMT	36
9	Mean wind and temperature for 16 November 1200 GMT	37
10	Mean normal wind component, V_j, for 16 November 1200 GMT	38
11	Magnitude of various terms in the heat balance equation, Eqn. (5), for 16 November 1200 GMT	43
12	Magnitude of the local temperature change for 16 November 1200 GMT	46
13	Magnitude of the estimated diabatic temperature change for 16 November 1200 GMT	46

TABLE OF SYMBOLS AND ABBREVIATIONS

A	area enclosed by lateral boundaries
B	index denoting averaging or integration to be performed along lateral boundaries
C_n	velocity component normal to the lateral boundary (+ inward)
C_p	specific heat of air at constant pressure
f	corillis parameter
F_s, F_n	frictional force in the s and n directions, respectively
g	acceleration of gravity
H	diabatic heating rate
J	Jacobian operator
K_M	mean kinetic energy measured with respect to the jet stream axis
l	length along the boundary B
n	coordinate direction oriented perpendicular to the jet stream axis
P_l, Pu	pressure at lower and upper boundaries of integration volume, respectively
R	gas constant for dry air
R_O	Rossby number
s	coordinate direction oriented along the jet stream axis
T	temperature
u_g, v_g	zonal and meridional components of geostrophic wind, respectively
u_j, v_j	wind components along and normal to the jet stream axis, respectively
α	specific volume

R/c_p

Φ geopotential

ψ stream function for horizontal wind

ω dp/dt

ACKNOWLEDGEMENT

The author wishes to thank Dr. J. D. Mahlman for his guidance and encouragement during the initial stages of this research. A special thanks is extended to Dr. R. L. Elsberry not only for his guidance and advice, but for what he taught this author about research and education in general. Lastly, the patience and moral support of my wife and children were greatly appreciated.

I. INTRODUCTION

Since the mid-1940's, when the existence of jet streams in the troposphere was documented by Rossby and Staff (1947), many studies of the Polar Front Jet Stream have been conducted. Notably, these studies have yielded a considerable amount of empirical knowledge about the Polar Front Jet. Unfortunately, the energetics of this jet are less well understood.

One important reason for this lack of understanding has been pointed out by Mahlman (1970). Considerable difficulty exists in defining an adequate curvilinear coordinate system for such a strongly time-dependent phenomenon. Some investigators have attempted to overcome this difficulty and have conducted studies of jet streams in curvilinear coordinates, with most interesting results. Riehl and Fultz (1957, 1958) in their steady, three-wave rotating dishpan experiment, investigated the dishpan jet stream in curvilinear coordinates, centered on the jet axis. They found net ascent poleward and net descent equatorward of the strong westerlies when averaging was performed around latitude circles. However, when the averaging was performed along the jet axis, the vertical circulation was reversed. This implied that the mean transverse circulation about the dishpan jet was thermally direct, while the mean meridional circulation in the same latitude operated in a thermally indirect sense. This suggested that the mechanisms responsible for maintaining the jet streams in a geographic coordinate system may be different from those in a curvilinear coordinate system.

The most detailed study of an atmospheric jet stream in curvilinear coordinates was performed by Krishnamurti (1961), on the subtropical jet stream, covering the period December 1955 and January-February 1956. The subtropical jet stream is particularly suitable to analysis in curvilinear coordinates since its day-to-day variability is rather small, especially when compared with the polar front jet. Krishnamurti's study also showed the existence of a thermally direct transverse circulation about the jet core. This agreed with the net transverse circulation about the jet in curvilinear coordinates. The mean meridional circulation in the latitudes of the subtropical jet operates in the same sense as the transverse circulation, in contrast to the dishpan jet.

The preceding studies avoided the time-dependent problem associated with jet streams. In the case of the dishpan jet the flow was in steady state with only longitudinal translation, and in the subtropical jet case the flow patterns were nearly stationary. In addition, both studies were limited to some extent, in that no explicit calculations of eddies in a curvilinear coordinate system were made.

Until recently no attempt has been made to extensively investigate the Polar Front Jet Stream in curvilinear coordinates since it is the most time-dependent of the major tropospheric jets. Mahlman (1970) minimized this time-dependent problem by choosing a Polar Front Jet where the time variations were not particularly large. While his study was quite extensive, it was limited primarily by two factors. First, an excessive amount of time was required to define the grid system, extract data, and perform the necessary calculations in the curvilinear coordinates. The second difficulty was in explicitly

computing eddy components of the wind in a curvilinear coordinate system. In this system an eddy quantity was defined as the value of a variable at a given point minus its mean value along the same line parallel to the jet axis. As Mahlman (1970) pointed out, in a curvilinear coordinate system, the system tends to be aligned nearly parallel to the flow. Thus, the computation of wind eddies was extremely sensitive to the orientation of the jet axis and small variations in the wind flow.

The first intent of this study was to develop a method for rapid, objective analysis of a jet stream. Meteorological input data was generated by a diagnostic-balanced, ω-equation program (Krishnamurti 1968), which required only geopotential heights. Thus both the divergent and nondivergent components of the wind are included in the study. Some discussion of the advantages and disadvantages of the data used, plus some steps necessary to minimize the disadvantages, is contained in Section II-B.

The objective computational scheme defined a coordinate along a jet stream axis and coordinate lines at distances 2.5 and 5.0 degrees latitude normal to the jet axis on either side (Fig. 1). Then the shceme linearly interpolated data from the various fields; ω,T,Φ,U and V components of the total balanced winds. The scheme calculated wind components normal and parallel to the jet axis. Line or area averaging, where appropriate, was performed to calculate the eddy components of variables. A detailed description of this scheme is contained in Section II-D.

Once the above computational scheme was developed, several checks were performed. First, results of the data interpolated from the initial data fields by the computational scheme were compared with

independent interpolations done by hand. Second, using the same time periods and jet axes at 300 mb that Mahlman (1970) used, the jet stream kinetic energy balance was calculated. The basic data fields and computational procedures were discussed by Mahlman (1970). The results obtained were then compared with Mahlman's results based on subjective interpolations and hand calculations.

The results of these checks were quite successful. Comparison of the data interpolated from the initial data fields by the computer and by hand showed very small differences, especially when averaged over the five time periods involved. This meant that the data interpolated by the objective scheme could be used with confidence in calculating the jet stream kinetic energy balance. Comparison of Mahlman's and the objective scheme calculations for the jet stream kinetic energy balance also showed good results which will be presented in Section IV.

Having satisfactorily developed the objective computational scheme, three further objectives for this research were set. First, due to certain inadequecies in the available data, which will be discussed in detail in Section II-B, jet axes at 200 mb were defined. The jet stream kinetic energy balance with respect to these axes was then calculated as it was for the axes at 300 mb mentioned previously. Second, since Mahlman's results were based on five time-period averages, it was felt that it would be of some interest to study a single time period. Therefore, the jet stream for 16 November 1200 GMT, 1966, was analyzed in detail. This period appeared to present the most explicit situation of a jet stream maximum of the five time periods studied.

Lastly, Mahlman (1970) discussed the role of eddy heat flux in the maintenance of the temperature structure about the jet. Mahlman's analysis indicated that eddy heat flux might counteract the expansion cooling and compression heating caused by the mean circulation about the jet. Therefore, the third objective of this research was to explicitly investigate the role of eddy heat flux in the maintenance of the temperature structure about a jet stream.

II. RESEARCH PROCEDURES

A. DESCRIPTION OF THE JET STREAM COORDINATE SYSTEM

The jet stream coordinate system for this project was defined, consistent with Mahlman (1970), in the following manner. A central coordinate was established, in this case, along the jet stream axis. Parallel coordinate lines were defined at distances 2.5 and 5.0 degrees latitude, normal to the jet axis in either direction. In an (s, n, p) curvilinear coordinate system, s and n were respectively the coordinates parallel and normal to the jet axis, and p was taken as the vertical coordinate. Separation between grid points along the s coordinates, other than the jet axis, was not uniform. This was the major difference between this grid and the one Mahlman used with uniform separation along all s coordinates. Once this jet stream-oriented coordinate system was defined by specifying an axis at a single pressure level, it is consistent through all levels in the vertical (See Fig. 1).

B. METEOROLOGICAL DATA USED

The case selected for analysis was an area centered over continental United States as described by Mahlman (1970). Data at five synoptic observation times was used, from 15 November 1200 GMT to 17 November

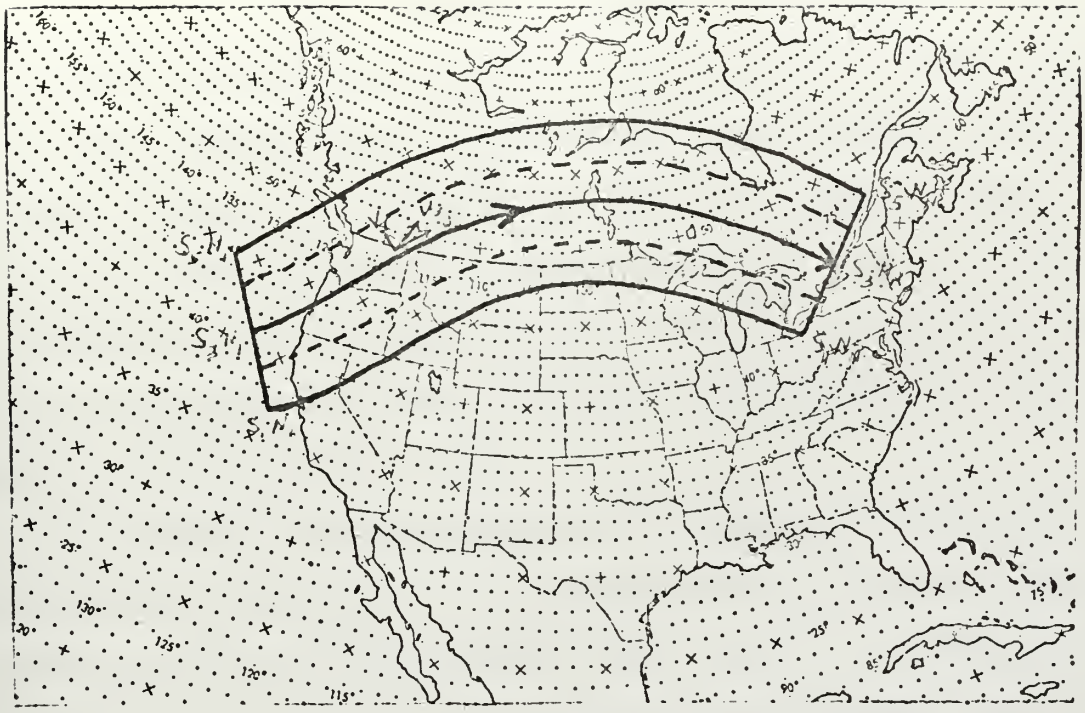

Fig. 1 Curvilinear grid for jet stream of 15 November 1966, 1200 GMT

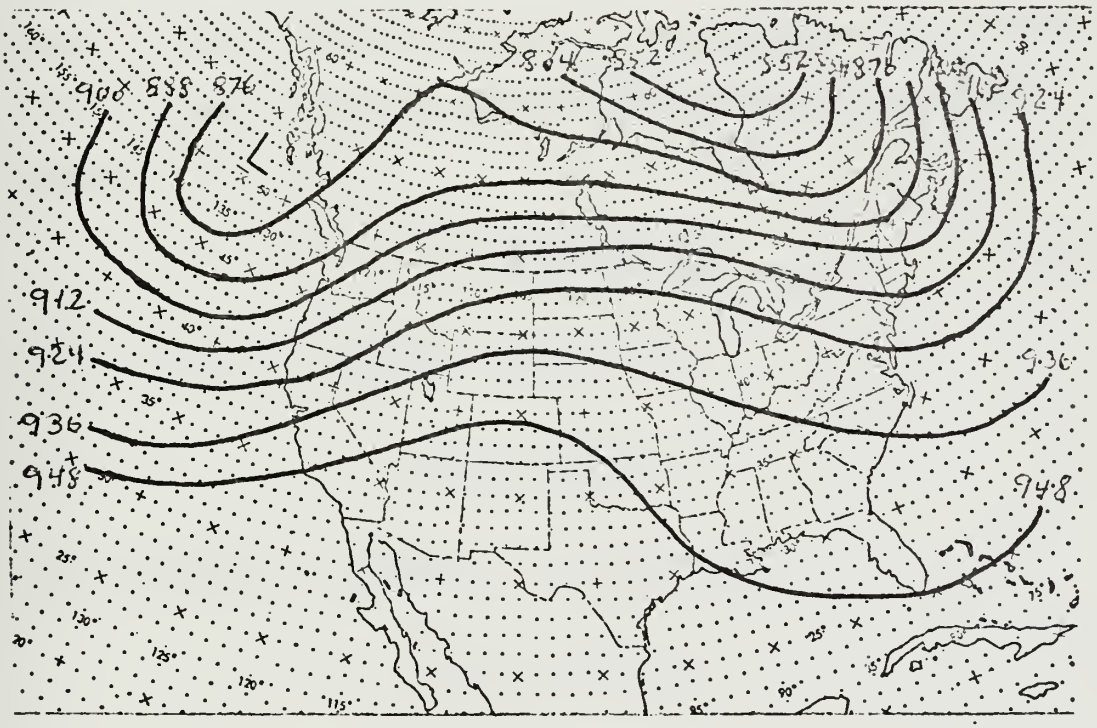

Fig. 2 Geopotential heights(m) at 300 mb on 15 November 1966, 1200 GMT

1200 GMT, 1966. During this period the flow at jet stream level was anticyclonic between troughs off the west coast and over Hudson Bay in the east. Although there was some change in the location of the jet stream, no significant development or large-scale system movement occurred. The jet stream axes did show a tendency to shift to the southeast with the jet maxima traveling eastward along the axis. Thus, this case appeared to present a satisfactory steadiness of the jet axis for analysis (See Fig. 2).

As mentioned in the introduction, all meteorological data in this research were generated by the diagnostic balance, ω-equation model, developed originally by Krishnamurti (1966, 1968). In this model, the equations are scaled for motions of characteristic Rossby number less than unit ($R_o<1$). Initial input data was obtained from the National Meteorological Center's objectively analyzed geopotential fields at 1000, 850, 700, 500, 300, and 200 mb. The stream function (ψ) was related to the geopotential field through the non-linear balance equation,

$$\nabla \cdot f \nabla \psi + 2J\left(\frac{\partial \psi}{\partial x}, \frac{\partial \psi}{\partial y}\right) = \nabla^2 \Phi \tag{1}$$

If the ellipticity condition for Eqn. (1)

$$\nabla^2 \Phi + 1/2 f^2 - \nabla f \cdot \nabla \psi > o \tag{2}$$

is not satisfied, then Eqn. (1) is replaced by

$$\nabla \cdot f \nabla \psi = \nabla^2 \Phi - 2J(u_\delta, v_\delta) \tag{3}$$

The meteorological data output was in staggered levels as shown in Fig. (5). Fields of ψ, Φ, and $\frac{\partial\psi}{\partial t}$ appear at the 1000, 800, 600, 400, and 200 mb levels, while ω, T, and Θ are given at the 900, 700, 500, 300 mb levels. The horizontal grid points were spaced 2.5 degrees latitude and longitude apart. The grid extends from 70W to 135W and from 25N to 60N. Six additional grid points in the zonal direction did not contain initial data, but were used to provide cyclic continuity for any given dependent variable. These grid point values were interpolated from values at the first two and last two of the grid points with real initial data. There was no staggering of variables in the horizontal. For a concise description of the computational procedures of this model, see Krishnamurti (1968) and Mahlman (1970).

Some limitations of the data have appeared. First, the jet stream chosen, while of moderate intensity, was not particularly well-defined. For most of the time periods, two distinct jet axes, whose separation was less than 10 degrees latitude, were present. During the last two time periods, 17 November 0000 GMT and 17 November 1200 GMT, 1966, a moderate jet stream associated with the low center over Hudson Bay impinged on the northeast corner of the grid, merging with the jet stream being analyzed. This caused some difficulty in defining axes and in interpreting the results. The manner in which this problem was handled is discussed in Section II-C.

Second, the ellipticity problem of the balance equation along with erroneous geopotential heights adjustments had to be considered. When the ellipticity condition for Eqn. (1) was not satisfied, Eqn. (3) was substituted for Eqn. (1). This adjustment was frequently required on

the anticyclonic side of the jet stream. Ellsaesser (1968) has compared the calculated winds of the balance equation with the observed winds. In places he found the mean jet stream at 300 mb was seventy percent stronger than indicated by the balance equation. Calculated wind speeds just equatorward of the jet stream were also found to be significantly lower. Calculations bear out this disadvantage of the non-linearized balance equation.

Errors in data handling also appeared. This problem was not particularly serious, since it was obvious when the error was large. Subjective adjustments to the geopotential heights were made when necessary.

Since it was not an objective of this research to analyze the balance equation model, no attempt was made to change the model to minimize the ellipticity problem. However, when interpreting the results this limitation was kept in mind.

Third, having the vertical motion defined at different levels than the kinetic energy and temperature is an obvious limitation. The vertical advection terms were calculated by linearly interpolating the values between levels. While not considered serious this problem must be kept in mind when interpreting the results.

C. DESCRIPTION OF JET STREAM AXES ANALYZED

For descriptive purposes the jet axes analyzed were divided into two groups, those based on observed winds and those based on the computed (balanced) winds. The first group used jet axes defined from the National Meteorological Center's maps of observed 300 mb winds and those were the ones used to compare with Mahlman's results.

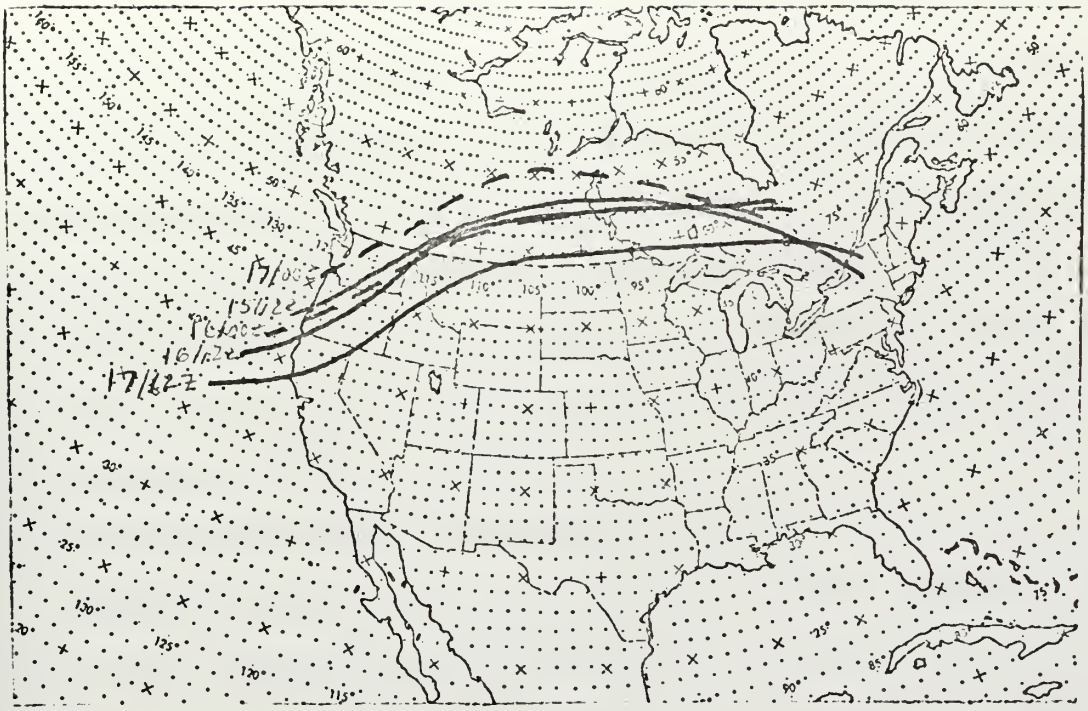

Fig. 3 Jet stream axes at 300 mb, defined from the observed winds

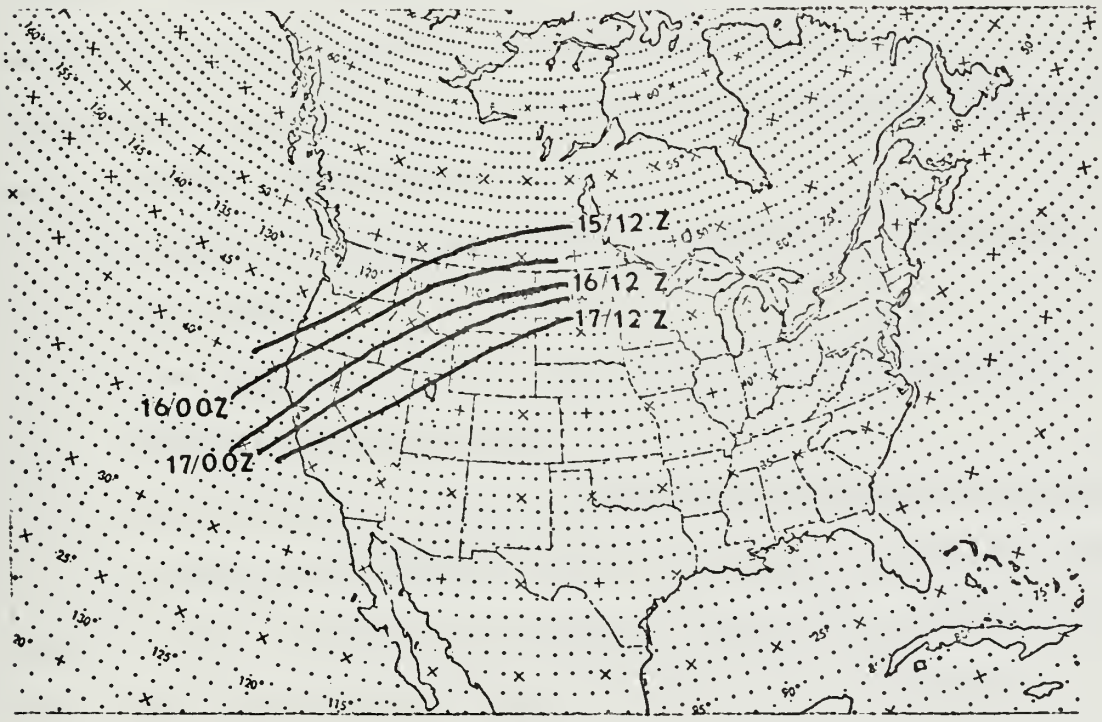

Fig. 4 Jet stream axes at 200 mb, defined from the total balanced winds

The second group used jet axes at 200 mb defined from balanced winds (See Fig. 4). The jet streams thus specified were of moderate strength, fairly well-defined, and presented a reasonable representation of the observed winds at 200 mb. Unfortunately, the definition of the jet stream axes was not particularly good east of 95W. Consequently, only that portion of the jet axes west of 95W was analyzed. These five axes gave a good picture of jet stream flow from SW to NE but only a half wave-length was being analyzed.

D. DESCRIPTION OF OBJECTIVE COMPUTATIONAL SCHEME

A computer program was developed for the IBM 360/67 system of the W. R. Church Computer Center which performed the calculations described in the following section. The remainder of this section is a general description of the computational scheme used. Primary emphasis is placed on operations performed and principles applied. The generality and flexibility of this program is also discussed in some detail. For a detailed discussion of the mechanics concerning how the operations were performed, see Appendix A.

The computer computational scheme was divided into four subroutines:

1. data input
2. development of the curvilinear grid to be superimposed on the geographic data fields at all levels
3. interpolation of data from geographic to curvilinear system
4. computations performed using a curvilinear coordinate system.

The data input subroutine was simply the reading of the initial data fields and the definition of the jet stream axis in geographic coordinates.

The curvilinear coordinate system developed in the next subroutine was a simple design (See Fig. 1). The points along the jet stream axis were located at two degree latitude intervals along the jet axis. Then, utilizing the slope of the jet axis at each point in a scheme described in Appendix A, grid points were established at 2.5 and 5.0 degrees latitude normal to the axis. The grid was constant for all levels in the vertical. The area enclosed by the curvilinear grid and the distance between grid points was also calculated.

Data was interpolated from the geographic grid to the curvilinear grid in the third subroutine. A linear interpolation in two-dimensions was used for this transformation. After the data was interpolated from geographic to curvilinear coordinate points, a linear interpolation in one-dimension (vertical) was performed to obtain values of ω and Θ between the staggered levels.

In the fourth subroutine with fields of temperature, vertical motion, geopotential heights, and the u and v components of the total balanced wind at the curvilinear grid points available, the first calculation was to convert the u and v wind components to components parallel and normal to the jet axis at each point. This is done by the scheme described in Appendix A, utilizing the jet axis slope. Next, the eddy components of each variable were calculated. Either a line or area averaging scheme, as appropriate, was used to obtain the mean of a variable along the coordinate. Then this mean was subtracted from the value of the variable at each point. Both eddy and mean values were required for the kinetic energy balance and the eddy heat flux calculations. To facilitate the discussion, the equations used and the results are discussed in Sections III and IV.

One of the advantages of this program was its generality and flexibility. This program was made general so that it might be used with other than polar-stereographic maps and 27 by 15 grid arrays. The program was flexible in that there is no restriction that the n coordinates be at 2.5 and 5.0 degrees latitude from that jet axis, or that there be only two coordinate lines on either side of the jet axis. The s coordinate lines were not limited to 2 degrees latitude distance along the axis. There may be any number of s coordinates, and of any interval length desired.

III. EQUATIONS

In this report, the averaging notation was that used by Mahlman (1970). The mean of an arbitrary quantity, Q, was given by $[Q]_{(s)}$. The subscript enclosed by small parentheses indicates the coordinates over which the averaging was performed. The deviation of Q from that average was given by (Q), i.e., $Q=[Q]_{(s)} + (Q)_{(s)}$ for averaging processes along the jet. When averaging normal to the jet, n was substituted for s.

Consistent with Mahlman (1970) the following equation was used to obtain the kinetic energy balance of the jet stream.

$$\frac{\partial}{\partial t}\int_{p_u}^{p_l} \frac{[u_J]^2_{(s)} + [v_J]^2_{(s)}}{2}(n)\,\frac{dp}{g} = \frac{\partial K_M}{\partial t} =$$

$$\overbrace{\qquad\qquad}^{(a_1)} \qquad \overbrace{\qquad\qquad\qquad}^{(a_2)}$$

$$+ \int_{p_u}^{p_l} \frac{1}{A_B} C_n \frac{[u_J]^2_{(s)} + [v_J]^2_{(s)}}{2}(n) + [u_J]_{(s)}(u_J)_{(s)} + [v_J]_{(s)}(v_J)_{(s)}\, d_1 \frac{dp}{g}$$

$$\overbrace{\qquad\qquad}^{(b_1)} \qquad \overbrace{\qquad\qquad\qquad}^{(b_2}$$

$$- \frac{\omega}{g} \frac{[u_J]^2_{(s)} + [v_J]^2_{(s)}}{2} + [u_J]_{(s)} (u_J)_{(s)} + [v_J]_{(s)} (v_J)_{(s)} \Big|_{(s,n)}^{p_1}$$

$$\overbrace{\qquad\qquad}^{(c_1)} \qquad \overbrace{\qquad\qquad\qquad}^{(c_2)}$$

$$+ \frac{\omega}{g} \frac{[u_J]^2_{(s)} + [v_J]^2_{(s)}}{2} + [u_J]_{(s)} (u_J)_{(s)} + [v_J]_{(s)} (v_J)_{(s)} \Big|_{(s,n)}^{p_u}$$

$$+ \int_{p_u}^{p_1} (u_J)_{(s)} (v_J)_{(s)} \frac{\partial}{\partial n} [u_J]_{(s)} \Big|_{(s,n)} + (u_J)_{(s)} (\omega)_{(s)} \frac{\partial}{\partial p} [u_J]_{(s)} \Big|_{(s,n)}$$

$$+ (v_J)^2_{(s)} \frac{\partial}{\partial n} [v_J]_{(s)} \Big|_{(s,n)} + (v_J)_{(s)} (\omega)_{(s)} \frac{\partial}{\partial p} [v_J]_{(s)} \Big|_{(s,n)} \frac{dp}{g}$$

$$+ \int_{p_u}^{p_1} [u_J]_{(s)} (f)_{(s)} (v_J)_{(s)} \Big|_{(s,n)} - [v_J]_{(s)} (f)_{(s)} (u_J)_{(s)} \Big|_{(s,n)} \frac{dp}{g}$$

$$+ \int_{p_u}^{p_1} \frac{[\Phi]_{(B)} - [\Phi]_{(s,n)}}{A} \Big|_B c_n \, d\ell \, \frac{dp}{g}$$

$$- \frac{1}{g} [\omega]_{(s)} \Big|_{(n)} [\Phi]_{(s)} \Big|_{(n)} \Big|_{(n)} \Big|_{p_1}$$

$$+ \frac{1}{g} [\omega]_{(s)} {}_{(n)} [\Phi]_{(s)} {}_{(n)} {}_{(n)} \Big|_{p_u}^{p_1}$$

$$- [\omega]_{(s)} {}_{(n)} [\alpha]_{(s)} {}_{(n)} {}_{(n)} \frac{dp}{g} \Big|_{p_u}^{p_1}$$

$$- [u_J]_{(s)} [F_s]_{(s)} + [v_J]_{(s)} [F_n]_{(s)} {}_{(n)} \frac{dp}{g} \Big|_{p_u}^{p_1}$$

The separate terms, labeled (a) through (j) have the following interpretation:

(a) flux of "mean" kinetic energy through the side boundaries;

(b), (c) flux of "mean" kinetic energy through the lower and upper boundaries, respectively;

(d) conversion of "eddy" kinetic energy to "mean" kinetic energy;

(e) an additional term in the conversion from "eddy" to "mean" kinetic energy which arises because the Coriolis parameter (f) varies along the axis over which the initial average is performed. It is interpreted as a conversion term because it appears with an opposite algebraic sign in the "eddy" kinetic energy equation;

(f) mean pressure interaction term at the side boundaries arising from energy conversion in an open system;

(g), (h) mean pressure interaction terms at the lower and upper boundaries, respectively;

(i) conversion of potential energy into "mean" kinetic energy due to mean transverse circulation about the jet core;

(j) dissipation of "mean" kinetic energy due to friction and sub-grid-scale mixing.

Mahlman specified that the "mean" kinetic energy balance in the symbolism implied in Eqn. (4) was:

$$\frac{\partial Km}{\partial t} = a, + b, + c, + f + g + h + i \quad - \quad \text{"dissipation:}$$

"Dissipation" was defined to be a combination of residual terms a_2, b_2, c_2, and j. The subscripts 1 and 2 referred to the mean and eddy values of a term respectively.

To investigate the role of eddy heat flux, the first law of thermodynamics was averaged along the jet axis and separated into mean and eddy components.

$$\frac{\partial [T]_{(s)}}{\partial t} = \overset{(1)}{- [v_J]_{(s)} \frac{\partial [T]_{(s)}}{\partial n}} \overset{(2)}{- \frac{\partial}{\partial n} [(v_J)_{(s)} (T)_s]_{(s)}}$$

$$\overset{(3)}{- \frac{1}{s_2 - s_1} u_J (T)_{(s)} \Big|_{s_2} - u_J (T)_{(s)} \Big|_{s_1}} \overset{(4)}{+ \frac{[H]}{c_p}_{(s)}}$$

$$\overset{(5)}{+ \frac{}{p} - \frac{\partial}{\partial p} (\omega)_{(s)} (T)_{(s)}}_{(s)} \overset{(6)}{+ [\omega]_{(s)} \frac{[\alpha]_{(s)}}{c_p} - \frac{\partial [T]_{(s)}}{\partial p}}$$

When discussing the results of calculations using the above equations, the alphabetic or numeric designations of terms are used. This is to simplify tables presented and to not have to continually repeat the meaning of terms.

IV. RESULTS

To facilitate discussion, the results of this research are presented in the following manner. First, section IV-A presents the results of the comparision between data interpolated from the initial data field by the computational scheme versus independent interpolation by hand. Second, sections IV-B and IV-C present the results of the calculation of the jet stream kinetic energy balance for the previously described axes at 300 mb and 200 mb (see Section II-C). Section IV-B also contains Mahlman's (1970) energy calculation for the 300 mb jet axes with the results of this research. Third, in section IV-D the analysis of the jet stream defined at 200 mb by the total balanced winds for 16 November 1200 GMT is presented in some detail. Both jet stream structure and calculations of kinetic energy are presented. Lastly, in section IV-E results are presented of the investigation to explicitly determine the role of eddy heat flux in the maintenance of the temperature structure about a jet stream. The conclusions drawn from these results are presented in section V.

A. COMPARISON OF INTERPOLATION METHODS

The results on the interpolation of the initial data fields from geographic to curvilinear grid points by both the objective and manual techniques are shown in Figs. 5, 6, and 7. Fig. 5 shows the mean vertical motion relative to the jet axis averaged over the five time periods. The number above each point was obtained by the objective scheme, the value in parentheses was obtained by hand interpolation. No difference was greater than 10×10^{-5} mb sec^{-1}, and at more than 50 percent of the locations the difference was less than 5×10^{-5} mb

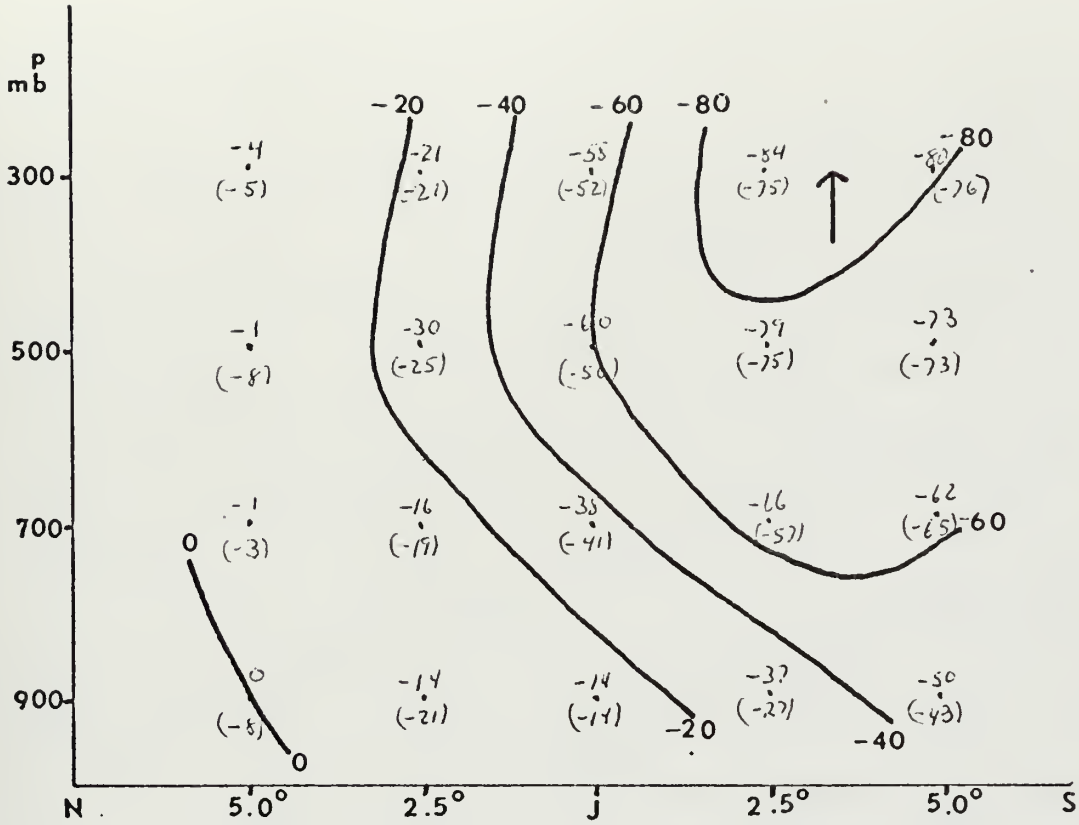

Fig. 5 Comparison of mean vertical motion ($[\omega]_{(s)}$, 10^{-5} mb sec^{-1}) interpolated by the objective scheme versus hand interpolation

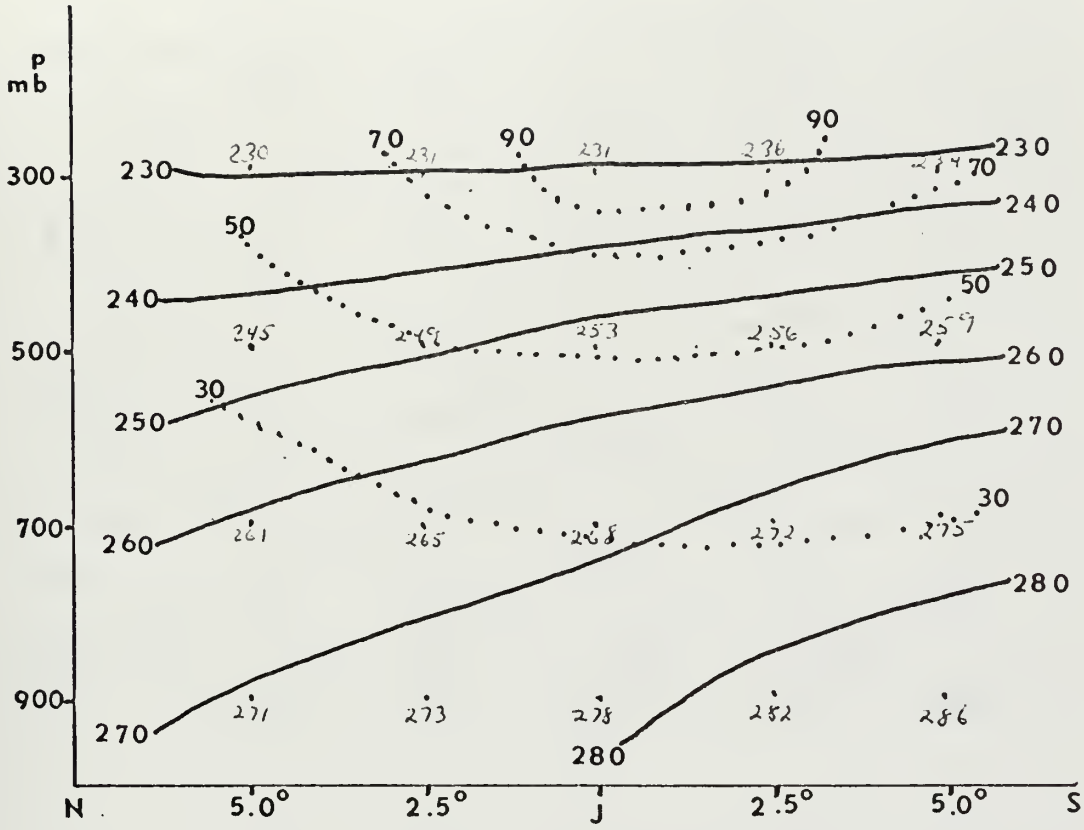

Fig. 6 Mean wind (knots) and temperature (deg K) calculated by the objective computational scheme

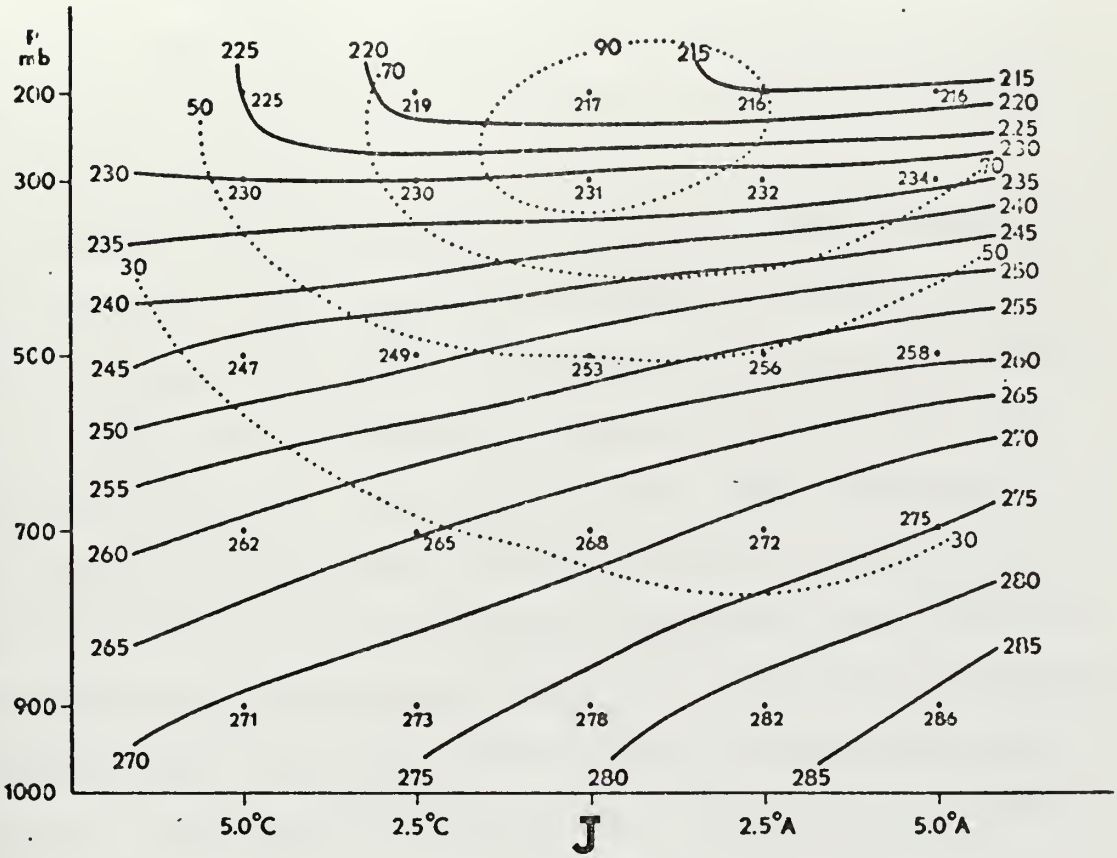

Fig. 7 Mean wind (knots) and temperature (deg K) along the polar front jet stream averaged from 15 November, 1200 GMT to 17 November 1200 GMT, 1966.

Mahlman(1970)

sec^{-1}. In the mean, the vertical motion field did not agree with Riehl and Fultz's (1957, 1958) finding of ascent equatorward and descent poleward of the jet axis (Section I). The first and last time periods did show ascent equatorward and descent poleward, but these results were cancelled out by ascending motion poleward of the jet axis during the other three time periods.

This difference in mean values is explained by the orientation of the jet axes used. Fig. 3 shows that the axes used did not cover an entire wavelength. They were predominantly in the region of a trough and of a ridge. This corresponds to regions of southerly flow and anticyclonic curvature. Riehl and Fultz (1957, 1958) found that for these specific regions, ascent occupied the area. Since these two regions were predominant in the averaging performed, ascent should be found throughout, being stronger equatorward. The ascending motion was somewhat stronger than Mahlman (1970) showed, but the patterns were the same. In both cases, ascending motion through the jet core was found.

Fig. 6 and 7 show the results for the mean wind (U_J) and temperature computed by the objective scheme and by Mahlman (1970) respectively. The mean winds were similar both in strength and pattern, and the mean temperatures were almost identical. Thus the results of this section indicate that the objective scheme gives comparable results to the manual scheme for interpolating data from geographic to curvilinear coordinate points.

B. KINETIC ENERGY CALCULATIONS FOR 300 MB JET AXES

The results for the 300 mb jet stream axes kinetic energy calculations for both the objective scheme and Mahlman (1970) are shown on Table 1. The calculations were performed from 100-900 mb over the area

defined by the curvilinear grid described in Section II. To acquire further insight, and enable more complete comparison with Mahlman's results, the volume was divided into regions below (300-900 mb) and above (100-300 mb) the jet. In addition, calculations of terms a_2, b_2, c_2, d and e of Eqn. (4) are included at the bottom of the table. This enabled some estimate to be made of eddy terms which Mahlman included as "dissipation". Although the results with the objective scheme were generally comparable with the hand-calculated values, there were some significant differences.

This was expected since the objective scheme used balanced winds and Mahlman used observed winds for kinetic energy computations. Where no horizontal wind calculations were involved, terms g and h, Eqn. (4), the results were almost identical. However, a definite difference existed, especially at upper levels, between terms where horizontal wind calculations were made, that is, terms $\frac{\partial Km}{\partial}$, a_1, b_1, c_1, anf f in Eqn. (4). Thus, the problems converning balanced winds discussed in section II-B must be considered when comparing these terms. The local change term ($\frac{\partial Km}{\partial t}$) best illustrated this problem, since it involved only u_J and v_J. Table 1 shows that for all layers the objective scheme results for $\frac{\partial Km}{\partial t}$ were lower than those calculated using observed winds. For this case this was in agreement with Ellsaesser's (1968) finding that balanced winds generally were lower than observed winds.

The role of the flux of mean kinetic energy and pressure interaction were the most significant differences between the two methods of calculations. In the 100-300 mb layer Mahlman's results show a net gain of +5.7 ergs $cm^{-2}mb^{-1}sec^{-1}$ versus the objective schemes net loss of

TABLE 1

	100 - 900 mb		300 - 900 mb		100 - 300 mb	
	MAHLMAN	OBJECTIVE	MAHLMAN	OBJECTIVE	MAHLMAN	OBJECTIVE
$\frac{\partial K_m}{\partial t}$	-5.1	-3.7	-10.6	-6.7	+11.2	+5.3
a_1	-0.8	-3.0	+0.3	+1.4	-3.9	-16.3
b_1	0.0	0.0	0.0	0.0	+9.6	+13.4
c_1	0.0	0.0	-3.2	-4.4	0.0	0.0
f	-1.8	-0.2	+0.2	+0.2	-8.0	-1.2
g	+0.2	+0.5	+0.2	+0.5	+14.3	+14.6
h	0.0	0.0	-4.8	-4.9	0.0	0.0
i	+1.9	+0.4	+3.0	+0.4	-1.3	+0.4
sum of terms $a_1 b_1 c_1$ f g h i	-0.5	-2.3	-4.3	-6.8	+10.7	+10.9
a_2		-1.5		-4.9		+8.9
b_2		0.0		0.0		-1.6
c_2		0.0		+0.5		0.0
d		+0.1		-0.4		+1.7
e		-1.1		-0.7		-2.1
sum of terms $a_2 b_2 c_2$ d e		-2.5		-5.5		+6.9
sum of all terms on right less j		-4.8		-12.3		+17.8
"implied" j		+1.1		+5.6		-12.5

Results of the contribution of terms in the kinetic energy balance equation, eqn. (4). All units expressed in erg cm mb sec

-2.9 ergs $cm^{-2}mb^{-1}sec^{-1}$for the flux of kinetic energy, terms a_1,b_1, and c_1 in Eqn. (4). The pressure interaction terms (f, g, and h) in Eqn (4), both show a net gain, +6.3 versus +13.4 ergs $cm^{-2}mb^{-1}sec^{-1}$.

For the 300-900 mb layer, however, the net results are very close. The flux terms a_1,b_1, and c_1, Eqn. (4) show a net loss in both cases, -2.9 versus -3.0 ergs $cm^{-2}mb^{-1}sec^{-1}$. The pressure interaction terms also showed almost identical net losses, -4.4 versus -4.2 ergs $cm^{-2}mb^{-1}sec^{-1}$.

The large difference in the upper layer 100-300 mb, had a biasing effect on the total layer (100-900 mb). For this layer the flux of kinetic energy was of the same sign, that is, a net loss, but the objective scheme's results were larger, -0.8 versus -3.0 ergs $cm^{-2}mb^{-1}sec^{-1}$. For the pressure interaction effects, the objective scheme shows a net gain, +0.3 ergs cm mb sec versus a net loss shown by Mahlman, -1.6 ergs $cm^{-2}mb^{-1}sec^{-1}$. Since terms b_1, c_1, g and h, Eqn. (4), gave essentially the same results, the terms a, and f, Eqn. (4), in the 100-300 mb layer were the primary difference.

These discrepancies were felt to be the result of the following differences. First, the objective scheme used balanced versus the observed winds used by Mahlman. Second, the objective scheme explicitly calculated V_J. Thus the calculations performed were affected by the jet axes to the south which effected this region (Section II-B). This effect was not considered by Mahlman (1970).

The results of the objective scheme and Mahlman's are comparable, if the problems mentioned above are considered. However, it does appear that the results of calculations using balanced winds at or near jet stream level are questionable.

The lower portion of Table 1 shows the calculation of eddy terms a_2, b_2, c_2, d, e and thus the implied value of dissipation. Calculation of these terms primarily involved using u_J and v_J, with the previously mentioned problems involved. Taking these problems into account, two findings concerning net results appear to be significant. First, the net value of the eddy terms is large enough to imply that these terms, a_2, b_2, c_2, d and e in Eqn. (4), do have an effect on the kinetic energy balance. Second, the residual term j in Eqn. (4) is of sufficient size to suspect that dissipation of mean kinetic energy due to friction and sub-grid-scale mixing does occur.

C. KINETIC ENERGY CALCULATIONS FOR 200 MB JET AXES

The results of the kinetic energy calculations using jet axes at 200 mb are shown in Table 2. As in the previous section, results are presented for a total layer and two sub-layers. The sub-layers, however, are different from those shown in Table 1. There were two basic reasons for this. First, the jet axes were at different levels, 200 mb versus 300 mb. Since the balance wind data was available only to 200 mb, it was impossible to calculate the wind in the region above 200 mb. Second, from the results of the comparison in section IV-B and the problems involved with the data (Section II-B), it was felt a different division of sub-layers was called for. Thus, the total layer was divided into two equal sub-layers, 500-900 mb and 100-500 mb. This took into account the apparent fact that balanced wind calculations in the vicinity of the jet stream were less reliable.

As shown in Table 2, one of the sifnificant results was the large value of the flux of mean kinetic energy through the side boundaries, term a_1, Eqn. (4), for the upper layer, 100-500 mb. It was large enough

TABLE 2

All units expressed in erg cm mb sec

	100-900 mb LAYER	500-900 mb LAYER	100-500 mb LAYER
$\frac{\partial K_m}{\partial t}$	-4.7	-5.0	-4.4
a_1	-14.5	+0.6	-29.6
b_1	0.0	0.0	+4.0
c_1	0.0	-4.0	0.0
f	-1.1	-0.2	-2.0
g	-0.1	-0.2	+0.5
h	0.0	-0.5	0.0
i	0.0	+0.1	-0.1
sum of terms $a_1 b_1 c_1$ f g h i	-15.7	-4.2	-27.2
a_2	+4.2	+2.5	+5.9
b_2	0.0	0.0	0.0
c_2	0.0	0.0	0.0
d	+0.3	+0.3	+0.3
e	+0.6	-0.5	+1.1
sum of terms $a_2 b_2 c_2$ d e	+5.1	+2.3	+7.3
sum of all terms on right less j	-10.6	-1.9	-19.9
"implied" j	+5.9	-3.1	+15.5

Results of kinetic energy calculations using eqn. (4) averaged over 5 days for jet axes defined from balanced winds at 200 mb.

to completely overshadow the net results both for that layer and the total layer, 100-900 mb. In the lower layer, 500-900 mb this dominance by term a_1, Eqn. (4) did not exist. In this layer the mean flux of kinetic energy through the upper boundary, term c_1, Eqn. (4) and the eddy flux of kinetic energy through the side boundaries, term a_2, Eqn. (4), had the dominant roles. For this layer, the mean and eddy terms almost cancelled, leaving a net -1.9 ergs $cm^{-2}mb^{-1}sec^{-1}$.

Results for the 200 mb jet axes were not directly comparable with the 300 mb axis. The balanced wind output tended to merge the two axes into a single axis closer to the northern axis in the first three time periods, and the southern axis in the last two periods. Furthermore, they covered only a half-wavelength. However, these results did allow for a check on the results presented in section IV-D of the jet stream at 200 mb for 16 November 1200 GMT.

D. ANALYSIS OF AN INDIVIDUAL JET STREAM AXIS

The results of the individual jet stream analysis are presented for the entrance and exit regions and are further sub-divided into a total layer and two sub-layers, 500-900 mb and 100-500 mb.

Fig. 8, 9, and 10 show the averaged vertical motion, temperature, and wind fields of both regions respectively. The results of the kinetic energy calculations for both regions are shown in Table 3. Table 3 also shows the result of averaging along the entire jet for use in making the comparison mentioned in section IV-C.

Considering the total jet structure first, vertical motion in the entrance region was ascending equatorward and descending poleward of the jet axis (Fig. 8). The normal wind, V_J, was equatorward below the jet defined at 200 mb (Fig. 10). Unfortunately, wind fields were not

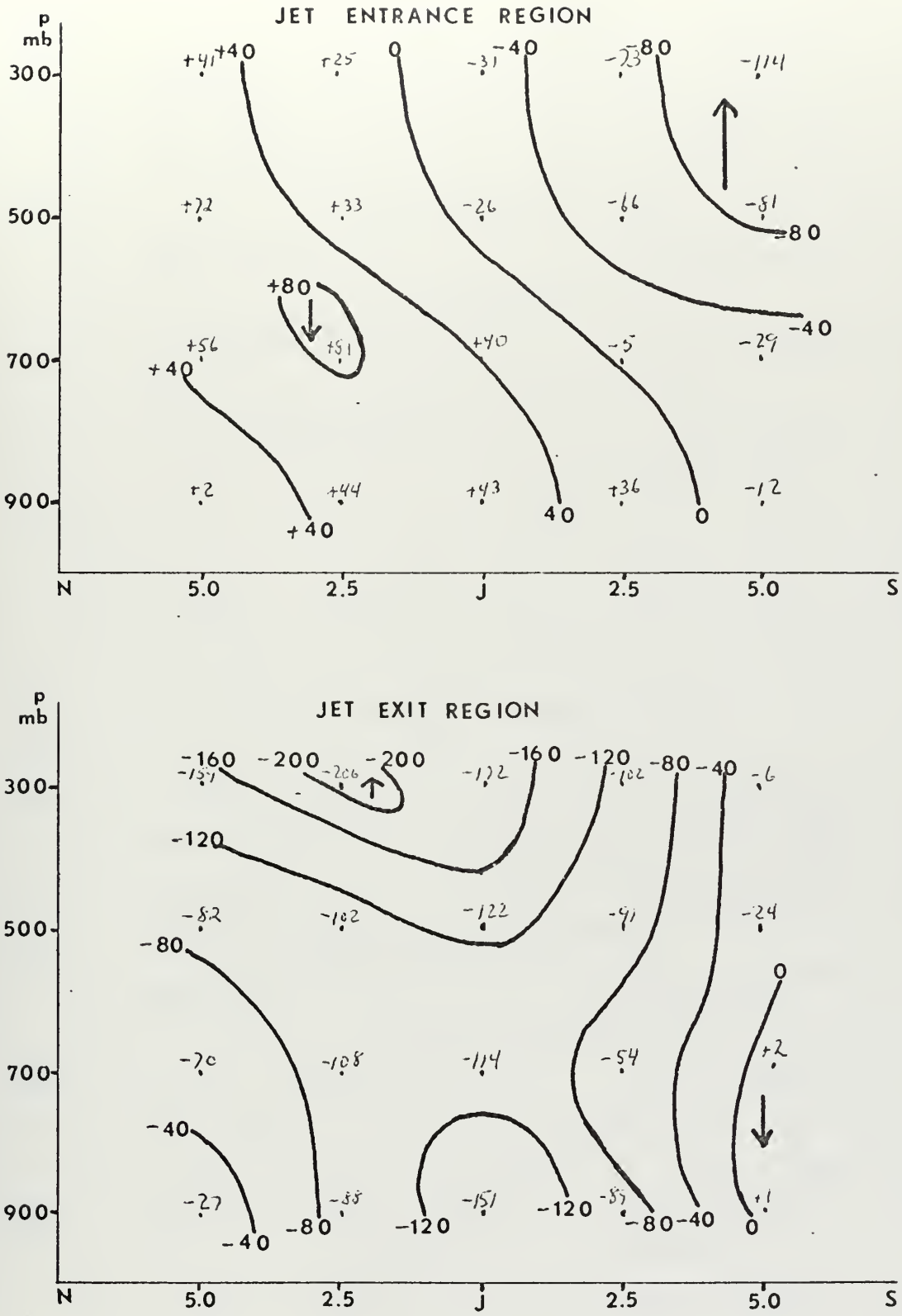

Fig. 8 Mean vertical motion ($[\omega]_s$, 10 mb sec^{-1}) for 16 November 1200 GMT

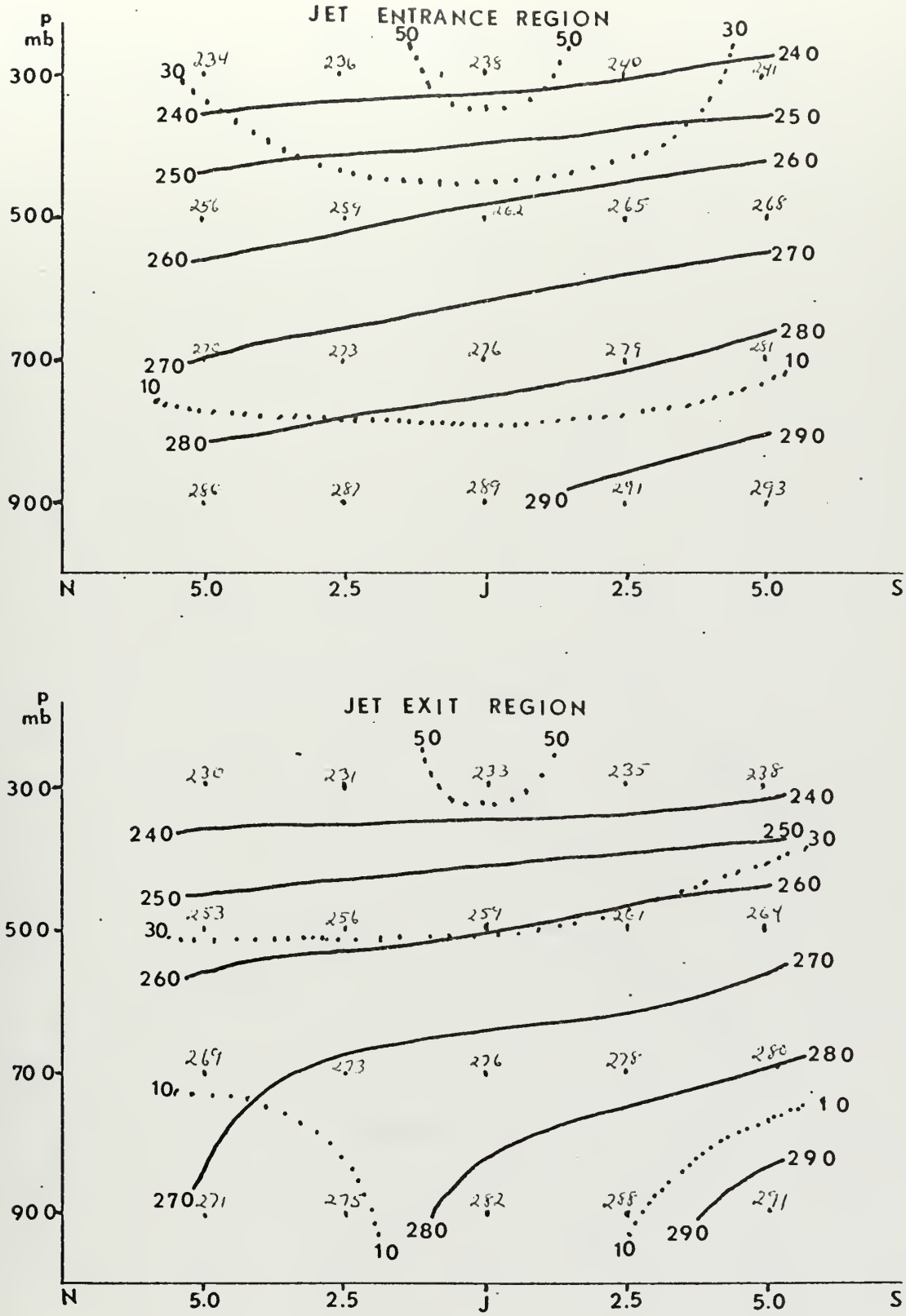

Fig. 9 Mean wind (m sec^{-1}) and temperature (deg K) for 16 November 1200 GMT

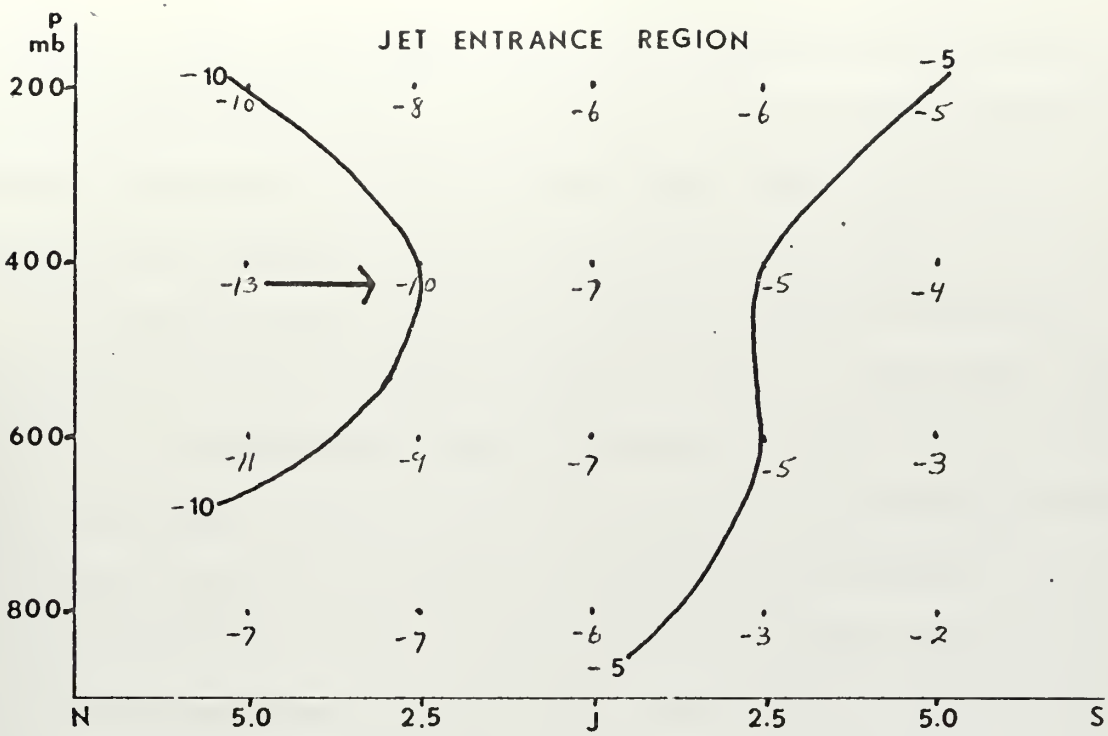

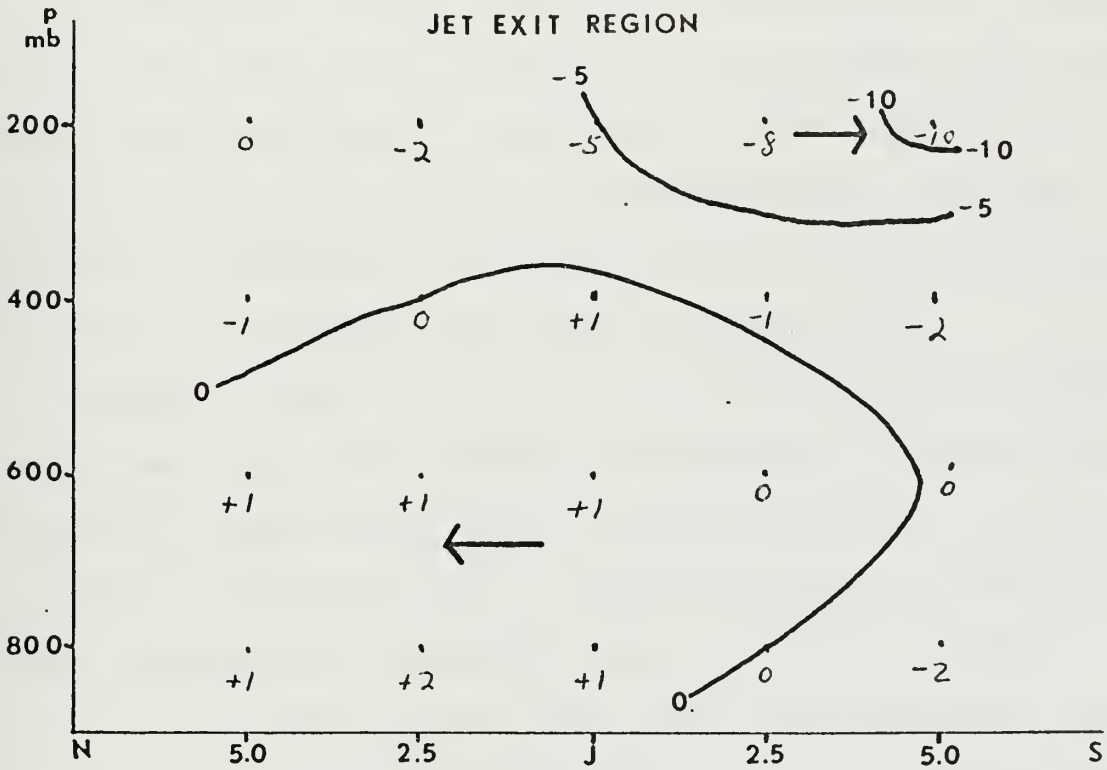

Fig. 10 Mean perpendicular wind, v (m sec)
for November 1200 GMT

available in the balance model above the jet stream level to check if the transverse winds there were poleward, thus completing a thermally direct circulation. In this region the normal winds, V_J, were considerably stronger than those found in the exit region.

The vertical motion in the exit region was ascending throughout, although much stronger poleward of the axis (Fig. 8). The normal wind field, V_J, did show some poleward flow beneath the jet, but the values were quite small (Fig. 10). Thus, an indication of a thermally indirect circulation did exist, but was not particularly well-defined. The large normal wind values south of the jet axis at jet stream level (Fig. 10), are attributed to the location of a jet stream to the south (see Section II-B and Section IV-B).

The temperature structure (Fig. 9), of the two regions is interesting. At jet stream levels, the entrance region is 3-5 K warmer than the exit region though the temperature patterns are the same. At 700 mb the temperatures for the two regions are almost identical. The large difference in temperatures poleward of the axis at 900 mb is attributed to a cold surface outbreak that occurred during this time.

As shown in Table 3, one of the most significant results again is the extremely large value, for the 100-500 mb layer, of the mean and eddy flux of kinetic energy through the side boundaries, terms a_1 and a_2, Eqn. (4), especially term a_2. Although large values had been found before, none had been comparable to term a_2, Eqn. (4), as shown in Table 3. These results were too large to be considered reliable, and could not be explained by the data problems discussed in Section II-B and IV-B.

TABLE 3

All units expressed in erg cm mb sec

	100 – 900 mb LAYER			500 – 900 mb LAYER			100 – 500 mb LAYER		
	JET ENT.	JET EXIT	ENTIRE JET	JET ENT.	JET EXIT	ENTIRE JET	JET ENT.	JET EXIT	ENTIRE JET
$\frac{\partial K_m}{\partial t}$			-15.3			-10.2			-20.7
a_1	-19.0	-4.2	-15.7	-0.8	+1.8	+0.5	-37.2	-10.1	-32.0
b_1	-0.1	+0.2	0.0	-0.1	+0.4	0.0	+0.4	+4.2	+3.3
c_1	0.0	0.0	0.0	-0.4	-4.2	-3.3	0.0	0.0	0.0
f	+1.7	-0.9	-0.2	+0.2	-0.4	-0.2	+3.3	-1.4	-0.2
g	+0.1	-0.3	0.0	+0.3	-0.6	+0.1	+5.6	-7.4	+1.5
h	0.0	0.0	0.0	-5.6	+7.4	-1.5	0.0	0.0	0.0
i	-0.7	+0.5	-0.1	-0.2	+0.1	-0.1	-1.1	+0.4	0.0
sum of terms $a_1 b_1 c_1 f g h i$	-18.0	-4.7	-16.0	-6.6	+4.5	-4.5	-29.0	-14.3	-27.4
a_2	-86.7	+50.9	-18.9	-11.0	+11.2	+1.2	-162.3	+96.3	-39.0
b_2	0.0	+0.1	+0.1	0.0	+0.2	+0.2	-0.1	+1.6	+0.4
c_2	0.0	0.0	0.0	+0.1	-1.6	-0.4	0.0	0.0	0.0
d	-3.1	+3.0	-0.2	-0.6	+1.2	+0.2	-5.6	+4.4	-0.6
e	-4.7	-2.3	+1.5	+1.3	-0.2	+0.5	-10.5	-4.6	+2.6
sum of terms $a_2 b_2 c_2 d e$	-94.5	+60.7	-17.5	-10.2	+10.8	+1.7	-178.8	+97.8	-36.6
sum of all terms on right less j	-112.5	+56.0	-33.5	-16.8	+15.3	-2.8	-207.8	+84.1	-64.0
"implied" j			+18.2			-7.4			+43.3

Kinetic energy calculations using eqn. (4) for 16 November 1200 GMT jet stream, defined from balanced winds at 200 mb

The fact that only a portion of a wavelength was analyzed, and that it was further sub-divided into entrance and exti regions, must be considered. The findings indicate results for a segment of a jet azis, and not the averaged results along an entire wavelength. The change of signs between regions, Table 3, indicates balancing between regions along the jet axis. Since in this case the wind acceleration is much stronger in the jet entrance than the deceleration in the exit zone at jet stream level, the regions should not be expected to completely balance. Notice that at lower levels, where acceleration and deceleration are about equal, the two regions almost balance.

Taking the above into consideration, two conclusions result. First, the lower layer, 500-900 mb, is below the area where shears are large, and the results of the objective scheme may be considered reliable. Second, in the 100-500 mb layer terms g, h, and i, Eqn. (4) do not contain horizontal wind calculations, and term f, Eqn. (4) only uses c_N. THus, some comparison of these terms between layers is possible.

In Table 3 the entire jet results are slightly different from the average of the two regions because of a 2° separation between entrance and exit regions caused when the grid was developed by the objective scheme. Notice that the entire jet results for the 500-900 mb layer are very close to those shown in Table 2, Section IV-C, for this layer. Since these results are for two different situations, it is reasonable to assume that the results for the entrance and exit regions are reliable.

Comparing the 500-900 mb layer jet entrance versus the jet exit region, it is interesting to note the change of signs. For every term calculated in Eqn. (4), except c_1, the algebraic sign changed between regions. In addition, the entrance region showed a net loss, while the exit region showed a net gain for all terms (-16.8 vs +15.3 ergs $cm^{-2}mb^{-1}sec^{-1}$).

In the jet entrance region, kinetic energy was lost primarily by mean pressure interaction through 500 mb and the eddy flux of kinetic energy through the side boundaries. The exit region's kinetic energy gain was also primarily caused by mean pressure interaction through 500 mb and the eddy flux of kinetic energy through the sides. But viewing the entire jet stream the upward transport by the mean pressure interaction in the entrance region is offset by downward transport in the exit region.

E. INVESTIGATION OF EDDY HEAT FLUX

This investigation was conducted on the same jet stream axis used in Section IV-D, and was divided into the same regions, jet entrance and exit zones. Fig. 11 shows the magnitudes of the terms in the heat budget equation, Eqn. (5), for both regions and at various levels. Since temperatures above 300 mb were not available from the balance model, only results for the region below 300 mb are shown. The vertical convergence of eddy heat flux and eddy adiabatic compression, term 5, Eqn. (5) was negligible and not included in Fig. 11. The diabatic temperature change, term 4, Eqn. (5) was not calculated, although some estimates of it were made and are discussed later in this section.

Mahlman (1970) suggested that the horizontal convergence of eddy heat flux, term 2, Eqn. (5) might counteract the expansion cooling and compression heating caused by the mean circulation about the jet. Fig. 11 shows that except for the region poleward of the jet axis at 400 and 600 mb, eddy heat flux does not have an appreciable effect. In the entrance region eddy heat flux was the smallest of the four terms and showed a slight net transfer of heat poleward.

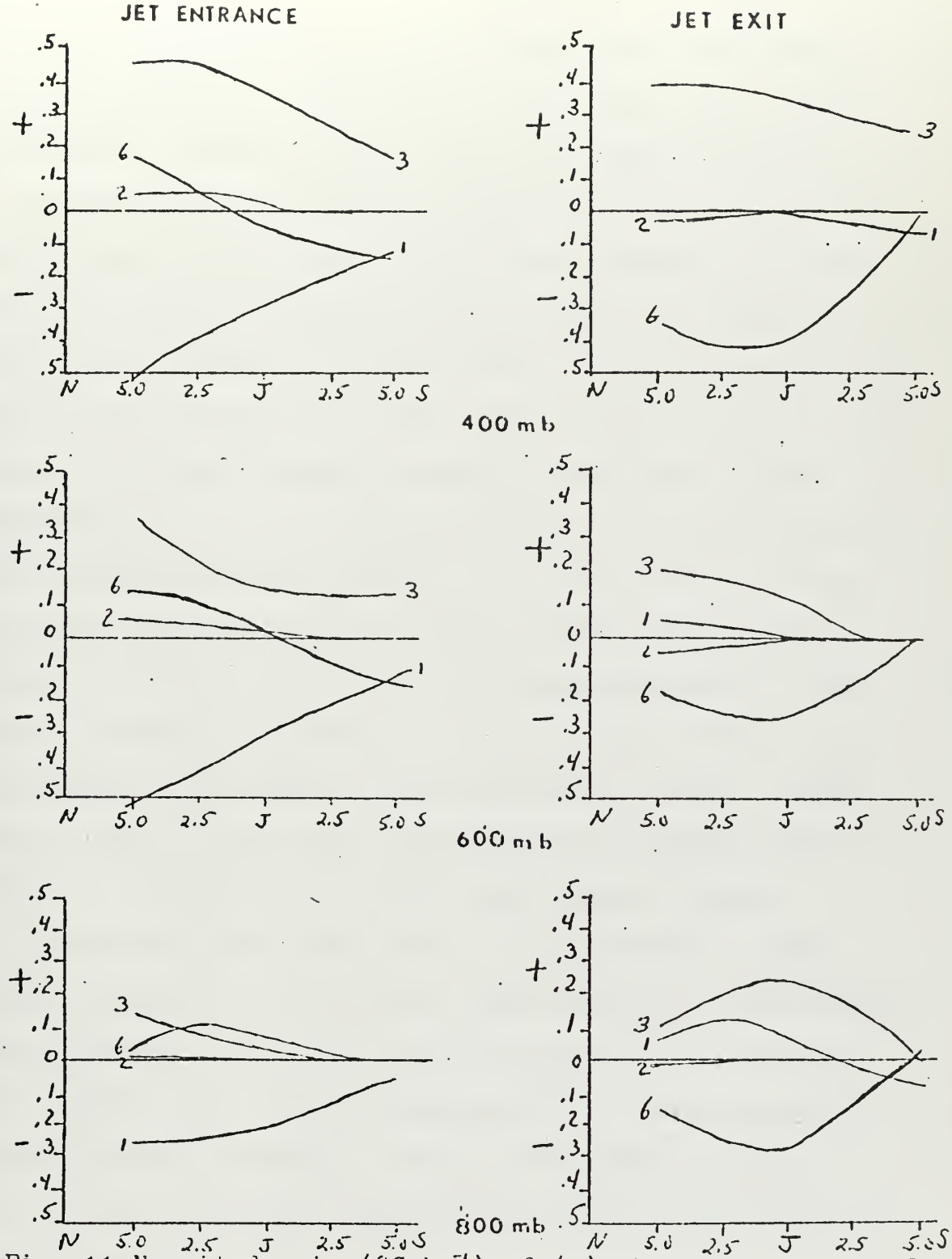

Fig. 11 Magnitudes in (°C hr⁻¹) of (1) the mean horizontal perpendicular advection, (2) "eddy" heat flux, (3)mean horizontal parallel advection, and (6) mean transverse vertical motion of the heat budget, eqn. (5) for the jet stream of 16 November 1200 GMT, defined from balanced winds

In the exit region the eddy heat flux was comparable in magnitude to the mean horizontal transverse advection, term 1, Eqn. (5), at both 400 and 600 mb. However, at these levels, both terms were small.

In the jet entrance region Fig. 11 shows that the mean horizontal advection terms (1 and 3, Eqn. (5)) were almost balanced. The cold advection of the mean horizontal normal advection, term 1, Eqn. (5), being slightly stronger than the warm advection of the mean horizontal parallel advection, term 3, Eqn. (5). In the jet exit region, the warm advection of the mean horizontal advection, term 3, Eqn. (5) was approximately balanced by the expansion cooling of the mean transverse vertical motion, especially poleward of and at the jet axis. In the jet entrance this balancing of the mean horizontal advection leaves the mean transverse vertical motion as primarily responsible for the warming poleward of the jet axis in the upper levels. The mean transverse vertical motion causes cooling equatorward of the jet. In the jet exit region, all the terms approximately balance except at 600 and 800 mb along the equatorward boundary, where cooling is shown.

An interesting point shown in Fig. 11 is the reversal of roles between jet regions by the horizontal normal advection and the vertical transverse motion. Notice that in the jet entrance, the mean transverse vertical motion pattern is approximately the same as the mean horizontal parallel advection. In the jet exit region the mean horizontal normal advection pattern closely follows the mean horizontal parallel advection.

The magnitudes of all terms shown in Fig. 11 decrease equatorward, except for the compression heating or expansion cooling due to mean transverse vertical motion, term 6, Eqn. (5), in the entrance region.

However, as Fig. 12 shows, the local change of temperature, $\frac{\partial [T]_{(s)}}{\partial t}$ is almost constant for all three levels across the jet. Thus, it is implied that to maintain this structure, the magnitude of the diabatic temperature change must increase equatorward. Fig. 13 shows that the estimated magnitude of the diabatic temperature change does increase equatorward, balancing the decrease equatorward of the other terms in Eqn. (5).

Confidence in the actual values of these results was limited. The temperatures used were computer generated and then interpolated to the same levels as the balanced winds. However, from the relative magnitude obtained, eddy heat flux did appear to play a role poleward of the jet axis. This agrees with Krishnamurti's (1961 b) findings for the subtropical jet that north of the jet axis there is an indication that heat flux is carried largely by daily eddies. The indication of this research is that the eddies do play a role in the heat flux, but not a dominant one. In addition, it appears that the diabatic temperature change equatorward of the jet axis plays a significant role.

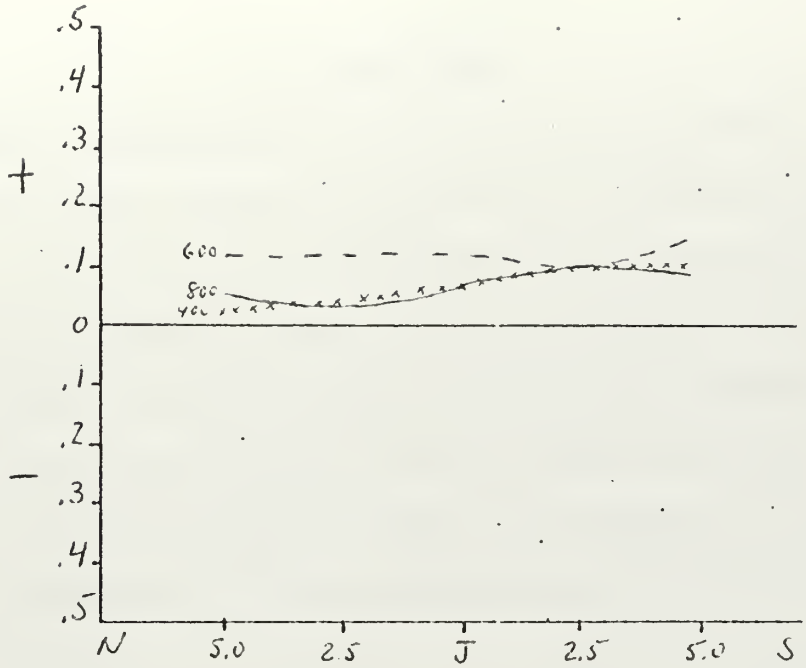

Fig. 12 Magnitude of the local temperature change eqn. (5) (in °Chr⁻¹) for 16 November 1200 GMT, for 800, 600, and 400 mb

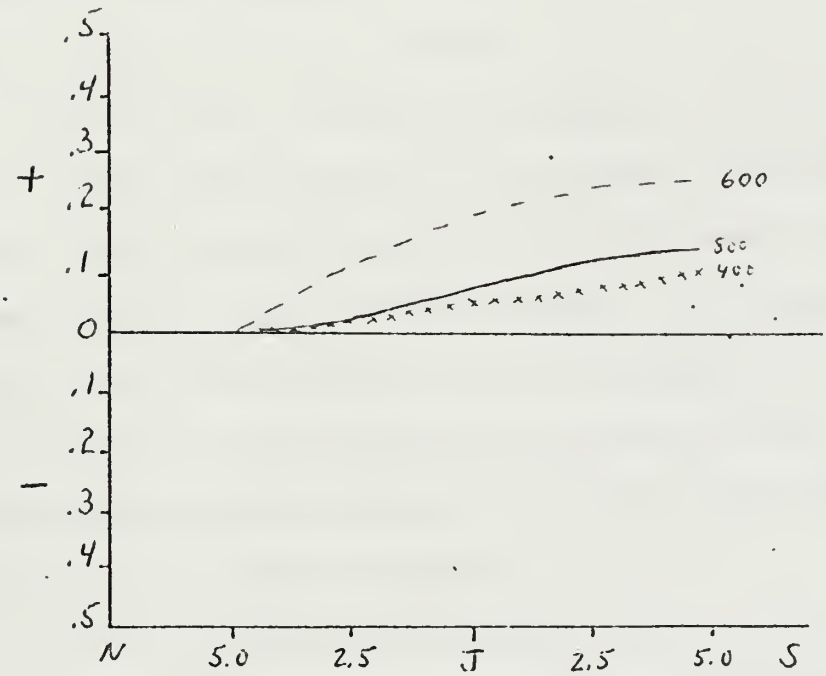

Fig. 13 Magnitude of the estimated diabatic temperature change, eqn. (5) (in °Chr⁻¹) for 16 November 1200 GMT, for 800, 600, and 400 mb.

V. CONCLUSIONS

Five valid conclusions are to be drawn from this research. First, the objective scheme developed did provide for a rapid and effective analysis of a jet stream. Wind computations in the vicinity of large wind shears may, however, require a finer grid than used. It is recommended that if wind computations are desired in large wind shear areas, the grid be small enough to resolve these large shears.

Second, use of total balanced winds in the vicinity of the jet stream are questionable. It is recommended that observed winds be used above 500 mb.

Third, there was a strong indication that the transverse circulation was thermally direct in the entrance zone and thermally indirect in the exit zone of a jet maximum. This was in agreement with the conclusions of Murray and Daniels (1953).

Fourth, kinetic energy is imported and exported from below the jet into the jet stream region primarily by the pressure interaction at 500 mb. This export and import along the axis is not seen if averaging is performed along the entire length of the axis. It is suggested that when studying jet stream energetics, the jet entrance and exit zones be included in addition to calculations along the entire length. It appears that some important features in maintaining a jet maximum tend to be balanced between these two regions.

Fifth, there was an indication that mean horizontal temperature advection and mean transverse vertical motion paly a significant role in the maintenance of the temperature structure poleward of the jet

axis. Equatorward of the jet axis there was a strong indication, from estimated results, that the diabatic temperature change plays a significant role in maintaining the thermal structure.

APPENDIX A

Throughout this report frequent reference to an objective computational scheme was made. A general description of the scheme was given in Section II-D, but specific details were not included. The purpose of this Appendix is to expand on the unusual concepts and geometry utilized in programming. It was not designed as a step by step analysis of the computer program nor as a discussion of concepts normally utilized in programming. However, for reference, a general list of arguments and arrays used is listed at the end of the Appendix.

The two concepts to be discussed are the establishment of the jet oriented grid system and the computing of wind components parallel and normal to the jet axis. In developing the concepts, for computational purposes, the two and a half degrees latitude and longitude between grid points were normalized to one. Thus, the jet axis grid points could be taken off the grid as if they were located on a normal rectangular x-y grid. Distance between grid points in the y-direction was 150 nautical miles. In the x-direction, distance was adjusted for each latitude by the formula: DX=DY *COS (PHI), with PHI equal to the latitude.

To determine the location of grid points 2.5 and 5.0 degrees latitude normal from the axis, the following scheme was used. First, the tangent at the individual jet axis grid point was determined. This was done by finding the distance in the x and y direction between the two jet axis grid points adjacent to the one used for calculation (see Fig. A-1). Using a computer library program ATAN 2 (A,B), the angle T was computed (Fig. A01). The sine and cosine of T, when added or

subtracted, as required, to the jet axis grid point, gives the location of the grid points 2.5 and 5.0 degrees latitude on either side of the axis. Repeating this operation at each grid point along the jet axis established the grid described in Section II-D.

To calculate the wind components normal and parallel to the jet axis, the angle T was used in conjunction with the u and v total balanced wind components at the curvilinear grid points. To obtain the parallel component, u was multiplied by cos T and v was multiplied by sine T. To get the normal component, u was multiplied by sin T and v was multiplied by sin T (Fig. A-2).

To assist any research in the future that might use this program, the following list of arguments and arrays is included. The complete program may be obtained from Dr. Russell L. Elsberry, Meteorology Department, Naval Postgraduate School, Monterey, California 93940.

NP = number of grid points along the jet axis.

NC = number of grid points along the jet axis minus one.

Used as a counter in DO-LOOPS

NF, ND, NL, or NR = number of levels in the vertical.

I = number of grid points along the Z or S-axis.

K = number of grid points along the X or S-axis.

J = number of grid points along the Y or M-axis.

L = number of grid points along the Y or M-axis.

TT = initial temperature field in degrees absolute.

UU = initial zonal component of the total balanced wind in m/sec.

VV = initial meridonal component of the total balanced wind in m/sec.

WW = initial vertical motion field in mb/sec times 10^5.

GP = geopotential height fields in meters.

PT = potential temperature.

A C in front of the above five values means that it was the value on the curvilinear grid.

PERVU = wind component normal to the jet axis.

PARVU = wind component parallel to the jet axis.

Any term with EDY before it designates an eddy value. All terms such as A1, A2, d, G, etc., refer to alphabetic designation given to various terms in equations discussed in the main part of this report.

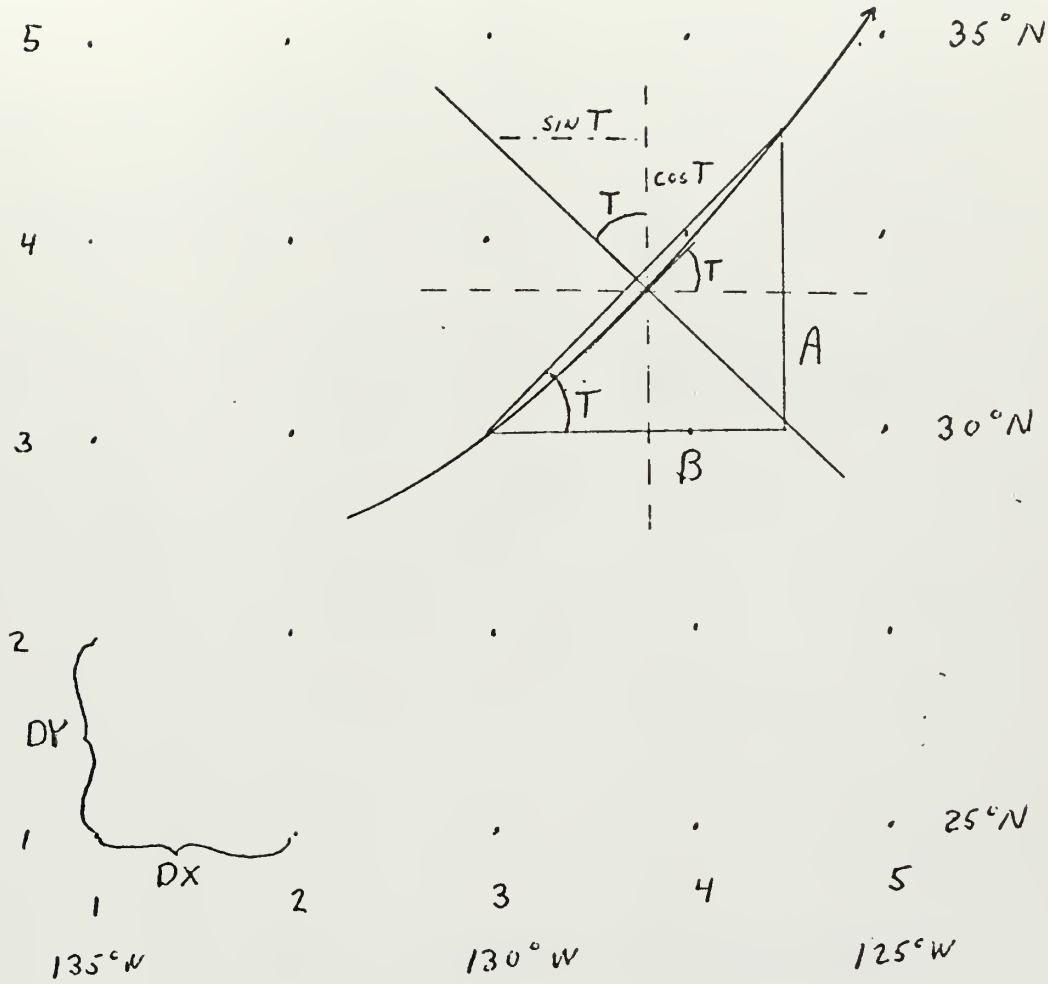

Fig. A-1 Schematic showing how angle T is calculated and used to define grid points

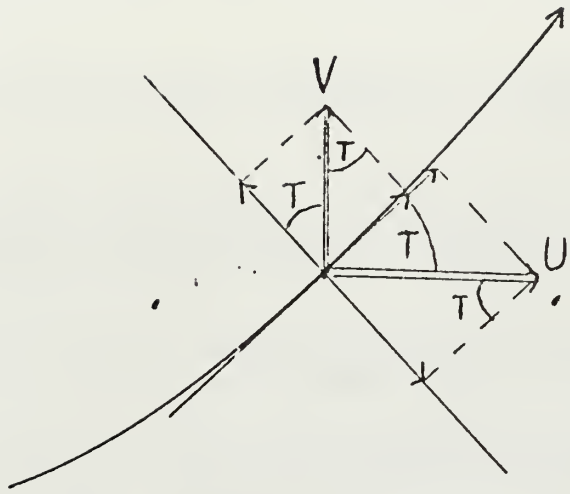

Fig. A-2 Schematic showing how angle T is used to acquire perpendicular and parallel wind components

BIBLIOGRAPHY

Ellsaeser, H. W., 1968: Comparative test of wind laws for numerical weather prediction. Monthly Weather Review, 96, 277-285.

Krishnamurti, T. N., 1961a: The subtropical jet stream of winter. J. Meteor., 18, 172-191.

_____, 1961b: On the role of the subtropical jet stream of winter in the atmospheric general circulation. J. Meteor., 18, 657-670.

Mahlman, J. D., 1970: Dynamical mechanisms producing large-scale transport of atmospheric trace substances. Research report, NPS-51MZ70101A, Naval Postgraduate School, Monterey, 45 pp.

Murray, R., and S. M. Daniels, 1953: Transverse flow at entrance and exits to jet streams. Quart. J. Roy. Meteor. Soc., 79, 236-241.

Riehl, H., and D. Fultz, 1957: Jet stream and long waves in a steady rotating dishpan experiment: structure of the circulation. Quart. J. Roy. Meteor. Soc., 83, 215-231.

_____, and _____, 1958: The general circulation in a steady rotating dishpan experiment. Quart. J. Roy. Meteor. Soc., 84, 389-417.

Rossby, C. G., and Staff Members, 1947: On the general circulation of the atmosphere in the middle latitudes. Bull. Amer. Meteor. Soc., 28, 255-280.

INITIAL DISTRIBUTION LIST

		No. Copies
1.	Defense Documentation Center Cameron Station Alexandria, Virginia 22314	2
2.	Library, Code 0212 Naval Postgraduate School Monterey, California	2
3.	Professor R. L. Elsberry Department of Meteorology Naval Postgraduate School Monterey, California 93940	5
4.	Lt. Robert F. Riordan, USN USS New Orleans (LPH-11) FPO San Francisco 94401	1
5.	Dr. J. D. Mahlman Geophysical Fluid Dynamics Laboratory/NOAA Princeton University P. O. Box 308 Princeton, New Jersey 08540	1
6.	Professor R. J. Renard Department of Meteorology Naval Postgraduate School Monterey, California 93940	1
7.	Professor F. J. Winninghoff Department of Meteorology Naval Postgraduate School Monterey, California 93940	1

Security Classification

DOCUMENT CONTROL DATA - R & D

(Security classification of title, body of abstract and indexing annotation must be entered when the overall report is classified)

1. ORIGINATING ACTIVITY (Corporate author)

Naval Postgraduate School
Monterey, California 93940

2a. REPORT SECURITY CLASSIFICATION

Unclassified

2b. GROUP

3. REPORT TITLE

An Analysis of Jet Stream Structure and Energetics Using an Objective Computational Scheme

4. DESCRIPTIVE NOTES (Type of report and inclusive dates)

Master's Thesis; March 1971

5. AUTHOR(S) (First name, middle initial, last name)

ROBERT FREDERICK RIORDAN

6. REPORT DATE

March 1971

7a. TOTAL NO. OF PAGES

57

7b. NO. OF REFS

8

8a. CONTRACT OR GRANT NO.

b. PROJECT NO.

c.

d.

9a. ORIGINATOR'S REPORT NUMBER(S)

9b. OTHER REPORT NO(S) (Any other numbers that may be assigned this report)

10. DISTRIBUTION STATEMENT

Approved for public release; distribution unlimited

11. SUPPLEMENTARY NOTES

12. SPONSORING MILITARY ACTIVITY

Naval Postgraduate School
Monterey, California 93940

13. ABSTRACT

An analysis of jet stream structure and energetics is performed utilizing an objective scheme that calculates wind components normal and parallel to the jet axis, with provisions to explicitly calculate the eddy components of variables. Most of the meteorological data used is generated by a diagnostic-balanced, ω-equation model. Results indicate that above 500 mb observed winds and temperatures should be used versus computer generated data.

There is some indication that between the jet entrance and exit regions the mean transverse vertical circulation reverses from thermally direct to thermally indirect. Kinetic energy is imported from below the jet into the jet stream region primarily by the mean pressure interaction at 500 mb.

Thermal balance calculations indicate that the mean horizontal temperature advection and vertical transverse motion are primarily responsible for maintenance of the temperature structure about a jet.

DD FORM 1 NOV 65 1473 (PAGE 1)

S/N 0101-807-6811

Security Classification

A-31408

Security Classification

14 KEY WORDS	LINK A ROLE	LINK A WT	LINK B ROLE	LINK B WT	LINK C ROLE	LINK C WT
Jet Stream						
Kinetic Energy Balance						
Heat Budget						

DD FORM 1 NOV 65 1473 (BACK)

S/N 0101-807-6821

Security Classification

A-31409

Thesis
R5728
c.1

136271

Riordan
An analysis of jet stream structure and energetics using an objective computational scheme.

thesR5728
An analysis of jet stream structure and
3 2768 001 91352 8
DUDLEY KNOX LIBRARY